Gibbs2: A new version of the quasi-harmonic model code. II. Models for solid-state thermodynamics, features and implementation.

A. Otero-de-la-Roza *, David Abbasi-Pérez and Víctor Luaña

Departamento de Química Física y Analítica, Facultad de Química, Universidad de Oviedo, 33006 Oviedo, Spain.
A contribution from the Malta-Consolider group (http://www.malta-consolider.com/).

Abstract

In this second article of the series, we present the GIBBS2 code, a Fortran90 reimplementation of the original GIBBS program [Comput. Phys. Commun. **158** (2004) 57] for the calculation of pressure-temperature dependent thermodynamic properties of solids under the quasiharmonic approximation. We have taken advantage of the detailed analysis carried out in the first paper to implement robust fitting techniques. In addition, new models to introduce temperature effects have been incorporated, from the simple Debye model contained in the original article to a full quasiharmonic model that requires the phonon density of states at each calculated volume. Other interesting novel features include the empirical energy corrections, that rectify systematic errors in the calculation of equilibrium volumes caused by the choice of the exchange-correlation functional, the electronic contributions to the free energy and the automatic computation of phase diagrams. Full documentation in the form of a user's guide and a complete set of tests and sample data are provided along with the source code.

PACS: 07.05.Bx, 71.15.-m, 64.10.+h 65.40.-b 64.30.Jk

Key words: Equations of State in Solids, Equilibrium Properties of Solids, Data Analysis, Treatment of Noisy Data, Discontinuous Data, Thermal Effects.

* Corresponding author
Email addresses: alberto@carbono.quimica.uniovi.es (A. Otero-de-la-Roza), david@fluor.quimica.uniovi.es (David Abbasi-Pérez), victor@carbono.quimica.uniovi.es (Víctor Luaña).

PROGRAM SUMMARY/NEW VERSION PROGRAM SUMMARY

Authors: A. Otero-de-la-Roza, D. Abbasi-Pérez and V. Luaña.
Program Title: GIBBS2.
Journal Reference:
Catalogue identifier:
Licensing provisions: GPL, version 3.
Programming language: Fortran90.
Operating system: Unix, GNU/Linux.
Number of processors used: 1.
Supplementary material: A set of tests, execution outputs and full documentation.
Classification: 7.8 Structure and Lattice Dynamics.
Nature of problem: Given the static $E(V)$ curve, and possibly vibrational information such as the phonon density of states, calculate the equilibrium volume and thermodynamic properties of a solid at arbitrary temperatures and pressures in the framework of the quasiharmonic approximation.
Additional comments: A detailed analysis concerning the fitting of equations of state has been carried out in the first part of this article, and implemented in the code presented here.
No. of bytes in distributed program, including test data, etc: 49 MByte.
No. of lines in distributed program, including test data, etc: 10906 lines of source code, 2287 lines of documentation (the pdf is 31 pages long), 156 lines of test inputs and 882209 lines in the test dataset.
Distribution format: tar.gz file.
External routines: Part of the minpack, pppack and slatec libraries (downloaded from `netlib.org`) are distributed along with the program.

LONG WRITE-UP

1 Introduction

The first principles calculation of accurate equations of state (EOS), thermodynamic properties and phase diagrams is a very useful tool in a number of fields, including geophysics[1] and materials research[2,3]. One of the main advantages of the calculation of pressure and temperature dependent crystal properties is the easiness with which extreme conditions, unattainable by experimental means, can be modeled. Indeed, provided that there are no technical difficulties (e.g. pseudopotential transferability issues[4]), pressure effects can be accounted for simply by compression of the calculated crystal geometry to smaller volumes. The inclusion of temperature effects, primarily related to the vibrational degrees of freedom inside the crystal, is more delicate. There are esentially two mainstream ways of incorporating temperature in a theoretical calculation: molecular dynamics simulations[5,6] and the quasiharmonic

approximation (QHA)[7]. The former is ideally suited for situations close to the classical limit, at temperatures close or including the melting temperature. The latter is based on the harmonic approximation and, as such, accurate only at temperatures of the order or below the Debye constant.

In this article, we present GIBBS2, a program that implements several varieties of the quasiharmonic approximation. The QHA has had in recent times a surge in popularity, thanks to the advent of very efficient methods of computing the vibrational dispersion relations of a crystal. In particular, the Density Functional Perturbation Theory[8] allows the calculation of phonon frequencies at a given crystal geometry using linear response theory. Nowadays, it is possible to undertake the prediction of equations of state and thermodynamic properties fully *ab initio* with breathtaking accuracy [9,10].

The GIBBS2 code is presented in this article as a successor of the highly popular GIBBS code[11,12], which has been completely rewritten from scratch. In the original GIBBS, emphasis was put on the calculation of thermodynamic properties from a minimal set of theoretical data, namely the static $E(V)$ curve, using a simplified Debye model to include temperature effects. In this new version, a number of models are implemented, with varying accuracy and input data requirements. The Debye model implemented in GIBBS is the least demanding and roughly the least accurate, requiring only the static energy curve, and possibly the Poisson ratio of the crystal. In the highest end of the accuracy scale, the full QHA has been implemented, requiring the user to input the phonon density of states (phDOS) or a mesh of phonon frequencies for each of the calculated crystal volumes. The different thermal models are discussed and compared in section 3.

A detailed analysis of the fitting techniques to static energy *versus* volume data has been carried out in the preceding article of this series[13]. Equivalent methods have been included in GIBBS2. With them, it is possible to generate error bars for calculated thermodynamic properties at arbitrary pressures and temperatures. The details of the fitting procedures are given in section 4.

A number of additional features have been implemented in GIBBS2, that are discussed in section 5. These include the calculation of other contributions to the free energy of the solid, such as the electronic free energy in metals, the implementation of empirical energy corrections (EEC) to account for known systematic trends in the calculation of equilibrium volumes and the automatic determination of phase transitions and phase diagrams.

In section 6, we discuss the structure of the code, its installation, usage and a complete input and output. The user interface of the original GIBBS has been made much easier to use, including the possibility of treating several crystal phases on the same run.

Table 1
Calculation parameters for magnesium oxide, diamond and fcc aluminum. The first field represents the number of volumes in the grid and E_{cut} is the plane-wave cutoff energy, in Ry. Next, we show the density of the electronic and vibrational meshes (Monkhorst-Pack), the electron configuration used to generate the pseudopotentials and the number of core electrons they represent.

	Vs	E_{cut}	$\boldsymbol{k}$-point	$\boldsymbol{q}$-point	El. config.	Core
MgO	174	80	$4 \times 4 \times 4$	$8 \times 8 \times 8$	Mg:$1s^2 2s^2 2p^6 3s^1$	2
					O:$1s^2 2s^2 2p^5$	2
C	31	60	$6 \times 6 \times 6$	$6 \times 6 \times 6$	$1s^2 2s^2 2p^2$	2
Al	43	50	$16 \times 16 \times 16$	$6 \times 6 \times 6$	$1s^2 2s^2 2p^6 3s^2 3p^1$	10

2 Computational details

In the following sections, we use three simple solids to discuss the features of GIBBS2: magnesium oxide, diamond and fcc aluminium. The calculations were carried out using a plane-wave plus pseudopotentials approach together with DFPT, as implemented in the Quantum ESPRESSO package[14]. Ultrasoft pseudopotentials for all the atoms were generated using the USPP program by D. Vanderbilt[15]. The phDOS was calculated for every volume point on a grid. The exchange-correlation functionals used were LDA and the PBE version of GGA. The calculation details are shown in table 1.

3 Thermal models

3.1 Introduction

The function controlling the geometry and phase stability of a solid under a given pressure and temperature is the non-equilibrium Gibbs free energy,

$$G^*(\boldsymbol{x}, V; p, T) = E_{\text{sta}}(\boldsymbol{x}, V) + pV + F^*_{\text{vib}}(\boldsymbol{x}, V; T) + F^*_{\text{el}}(\boldsymbol{x}, V; T) + \dots \quad (1)$$

where E_{sta} is the static energy (obtained directly from the *ab initio* calculation) and F^*_{vib} is the non-equilibrium vibrational Helmholtz free energy. The crystal structure is completely determined by the volume V, and a number of coordinates, including atomic positions and cell parameters, which we label collectively as $\boldsymbol{x}$. More free energy terms are used to represent additional degrees of freedom in the solid: electronic (F^*_{el}), magnetic, configurational, defects,...

The central result related to G^* is the following: at a given pressure (p) and temperature (T), the equilibrium geometry is achieved by minimizing G^* with respect to the remaining variables:

$$G(p,T) = \min_{\boldsymbol{x},V} G^*(\boldsymbol{x},V;p,T), \tag{2}$$

which yields equilibrium internal coordinates, $\boldsymbol{x}(p,T)$, and volume, $V(p,T)$, as well as the equilibrium Gibbs function $G(p,T)$. Because of the difficulty of calculating G^* for the whole potential energy surface, a usual approach is restricting the internal variables to those resulting of a minimization of the static energy at any given volume:

$$\boldsymbol{x}_{\rm opt}(V) \quad \text{from} \quad E_{\rm sta}(V) = \min_{\boldsymbol{x}} E_{\rm sta}(\boldsymbol{x},V), \tag{3}$$

that transforms equation 1 into:

$$G^*(V;p,T) = E_{\rm sta}(\boldsymbol{x}_{\rm opt},V) + pV + F_{\rm vib}(\boldsymbol{x}_{\rm opt},V;T) + \ldots \tag{4}$$

Minimization of the above equation with respect to volume yields the mechanical equilibrium condition:

$$\frac{\partial G^*}{\partial V} = 0 = -p_{\rm sta} + p - p_{\rm th} \tag{5}$$

where $p_{\rm sta} = -dE_{\rm sta}/dV$ is the static pressure, $p_{\rm th} = -\partial F^*_{\rm vib}/\partial V$ is the thermal pressure and p is the applied external pressure.

Using $\boldsymbol{x}_{\rm opt}$, instead of $\boldsymbol{x}(p,T)$, in the context of the QHA leads to what other authors have called the statically constrained QHA[16]. This approximation implies assuming that the effect of temperature is expressed through a thermal pressure instead of a thermal stress tensor, and that the free atomic coordinates are determined by the cell volume alone. The consistent computation of $\boldsymbol{x}(p,T)$ requires the knowledge of portions of the multidimensional potential energy surface and its associated vibrational properties. This approach is, in general, exceedingly expensive. Note that, because of Neumann's principle, thermal stress in cubic crystals is isotropic, so the test cases we present are free from the static constrain error.

3.2 The quasiharmonic approximation

In the harmonic model, the vibrations in a crystal are treated as a gas of $3nN$ non-interacting phonons with volume independent frequencies ω_i, where n is the number of atoms per primitive cell and N the number of cells in the macroscopic solid. The complete lack of anharmonicity in this model leads to

well known unphysical behavior[17]: zero thermal expansion, infinite thermal conductivity,... The simplest way of accounting for anharmonic effects is assuming the harmonic approximation at any given crystal geometry, even if it does not correspond to the equilibrium structure: the quasiharmonic approximation (QHA). Plenty of examples of the success of QHA in the prediction of thermodynamic properties and phase stability of solids can be found in the literature[18–21].

In QHA, the non-equilibrium Helmholtz free energy is (atomic units are used throughout the article):

$$F^*_{\text{vib}}(\boldsymbol{x}, V; T) = \sum_{j=1}^{3nN} \left[\frac{\omega_j}{2} + k_B T \ln\left(1 - e^{-\omega_j / k_B T}\right) \right] \tag{6}$$

$$F^*(\boldsymbol{x}, V; T) = E_{\text{sta}}(\boldsymbol{x}, V) + F^*_{\text{vib}}(\boldsymbol{x}, V; T), \tag{7}$$

where the vibrational frequencies ω_j depend on the crystal geometry $(\boldsymbol{x}, V)$. The considered solid is periodic with n atoms per primitive cell and a total of N cells, hence the limit of the summation. It is usual practice to measure extensive thermodynamic quantities per unit cell (F^*_{vib}/N in the equation above). Also, it is not possible to calculate a sampling of the vibrational frequencies comparable to the number of cells of a finite crystal. Instead, a relatively fine sampling of the first Brillouin zone is used, and it is assumed that each reciprocal space point represents a certain volume. This amounts to choosing a frequency normalization so that

$$3n = \sum_j \omega'_j, \tag{8}$$

and

$$\frac{F^*_{\text{vib}}}{N} = \sum_j \left[\frac{\omega'_j}{2} + k_B T \ln\left(1 - e^{-\omega'_j / k_B T}\right) \right], \tag{9}$$

where the index j runs over the number of calculated frequencies. In the following, we will drop the primes of the vibrational frequencies and we will assume that extensive quantities are calculated per primitive cell.

Summations over frequencies such as in equation 6 can be calculated by integration using the phDOS:

$$g(\omega) = \frac{dG}{d\omega} \quad ; \quad G(\omega) = \int_0^{\omega} \sum_{j=1}^{3nN} \delta(\omega - \omega_j) d\omega \tag{10}$$

$$F^*_{\text{vib}} = \int_0^{\infty} \left[\frac{\omega}{2} + k_B T \ln\left(1 - e^{-\omega / k_B T}\right) \right] g(\omega) d\omega. \tag{11}$$

The normalization condition (eq. 8) transforms into:

$$3n = \int_0^\infty g(\omega) d\omega, \tag{12}$$

so that extensive quantities are, again, calculated per primitive cell. The two approaches—using the ω_j calculated on a grid or the phDOS—have been incorporated into GIBBS2, and yield equivalent results.

Figure 1 shows the calculated phDOS for MgO, diamond and fcc aluminium. Aluminium contains only one atom per primitive cell, and so its dispersion relations are composed exclusively of the acoustic branches. MgO and diamond have 2 atoms per cell, so there are 3 optic and 3 acoustic branches in the dispersion diagram. The phDOS of diamond stretches to higher frequencies, because of the stiffness of the carbon-carbon covalent bond. The LDA and PBE phDOS show comparable features, and can be brought to almost coincidence by scaling. This is important, because it is the same effect observed when the volume is changed, indicating that the discrepancy between both functionals can be corrected by an appropriate modification of the equilibrium volume.

In a typical QHA calculation, the user inputs a volume grid together with the static energy $E(V)$ resulting from the minimization of the internal coordinates $\boldsymbol{x}$. In addition, either the frequencies or the phonon density of states at each volume are also provided. With this information, GIBBS2 loops over a list of user-controlled pressure-temperature pairs. For the chosen temperature, three quantities are calculated on the input volume grid: the static energy, the non-equilibrium Helmholtz free energy and the entropy, and fitted using the techniques described in the previous article[13] and summarized in the next section. The fit to F^* is used to find the equilibrium volume, $V(p,T)$, according to equation 5, where $p_{\rm sta} + p_{\rm th}$ is obtained as a $-\partial F^*/\partial V$. It is interesting to note that, should the vibrational frequencies be given in the input, the thermal pressure can also be calculated as:

$$p_{\rm th} = -\frac{\partial F^*_{\rm vib}}{\partial V} = -\sum_j \left[\frac{\omega_j \gamma_j}{2V} + \frac{\omega_j \gamma_j / V}{e^{\omega_j / k_B T} - 1} \right], \tag{13}$$

where $\gamma_j = -\partial \ln \omega_j / \partial \ln V$ are the mode gammas. This approach is, however, less general, because the mode gamma information is lost if only the $g(\omega; V)$ are given, and also less efficient, because it involves the fitting of each volume dependent frequency $\omega_j(V)$.

Once the equilibrium volumes are known, a number of thermodynamic properties are derived directly from F^* (equation 7). Namely, the equilibrium entropy (S), Helmholtz free energy (F), Gibbs free energy (G), internal energy (U),

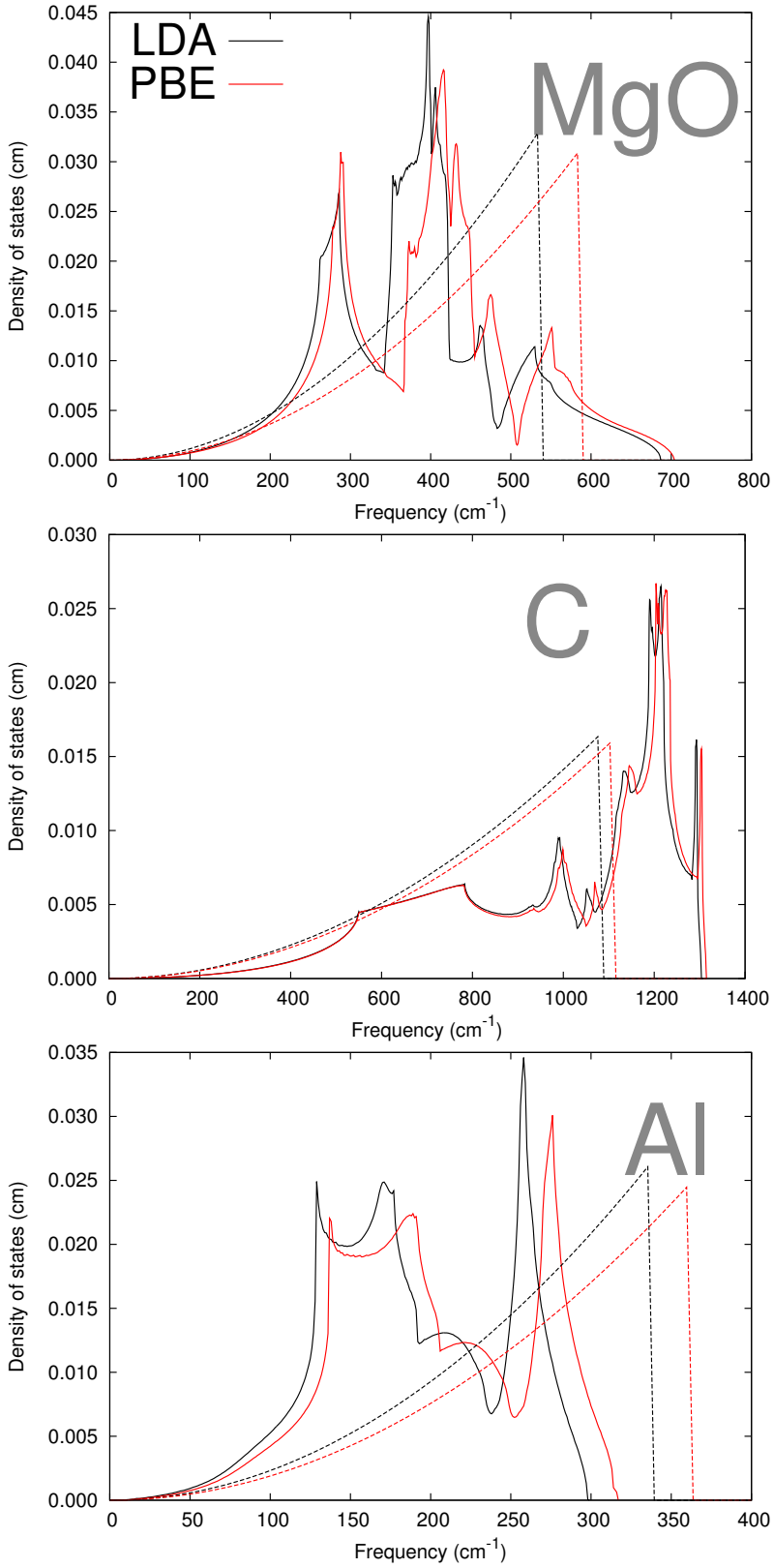

Fig. 1. Phonon density of states of MgO, diamond (C) and fcc Al, calculated using DFPT, with LDA (black) and PBE (red) exchange-correlation functionals at the experimental volumes. The phDOS used in the Debye-Slater model (see section 3.3 are represented with dashed lines.

constant-volume heat capacity (C_v) and isothermal bulk modulus (B_T):

$$F = F^*(V(p,T),T) \tag{14}$$

$$S = S(V(p,T),T) = -\left(\frac{\partial F}{\partial T}\right)_V = \sum_j \left[-k_B \ln\left(1 - e^{-\omega_j/k_BT}\right) + \frac{\omega_j}{T}\frac{1}{e^{\omega_j/k_BT}-1}\right] \tag{15}$$

$$U = U(V(p,T),T) = F + TS = E_{\text{sta}} + \sum_j \frac{\omega_j}{2} + \sum_j \frac{\omega_j}{e^{-\omega_j/k_BT}-1} \tag{16}$$

$$G = U + pV - TS \tag{17}$$

$$C_v = C_v(V(p,T),T) = \left(\frac{\partial U}{\partial T}\right)_V = \sum_j C_{v,j} = \sum_j k_B \left(\frac{\omega_j}{k_BT}\right)^2 \frac{e^{-\omega_j/k_BT}}{\left(e^{-\omega_j/k_BT}-1\right)^2} \tag{18}$$

$$B_T = -V\left(\frac{\partial p}{\partial V}\right)_T = V\left(\frac{\partial^2 F}{\partial V^2}\right)_T. \tag{19}$$

A second set of properties depend on the thermodynamic Grüneisen ratio:

$$\gamma_{\text{th}} = \frac{\alpha B_T V}{C_v}, \tag{20}$$

where α is the volumetric thermal expansion coefficient. In the quasiharmonic approximation, it can be computed using:

$$\gamma_{\text{qha}} = \frac{\sum_j \gamma_j C_{v,j}}{C_v}. \tag{21}$$

However, as in the calculation of p_{th}, it is preferable to avoid the computation of mode gammas. In this case, we use the thermodynamic relation:

$$\alpha B_T = \left(\frac{\partial S}{\partial V}\right)_T = \left(\frac{\partial p}{\partial T}\right)_V, \tag{22}$$

so we can use the volume derivative of $-TS$ to compute γ_{th}:

$$\gamma_{\text{th}} = -\frac{V}{C_v T}\left(\frac{\partial(-TS)}{\partial V}\right)_T. \tag{23}$$

Once the Grüneisen ratio is known, the thermal expansion coefficient, constant-

heat capacity (C_p) and adiabatic bulk modulus (B_S) follow:

$$\alpha = -\frac{1}{V}\left(\frac{\partial V}{\partial T}\right)_p = \frac{\gamma_{\rm th} C_v}{V B_T} \tag{24}$$

$$C_p = \left(\frac{\partial H}{\partial T}\right)_p = C_v(1 + \gamma_{\rm th}\alpha T) \tag{25}$$

$$B_S = -V\left(\frac{\partial p}{\partial V}\right)_S = V\left(\frac{\partial^2 U}{\partial V^2}\right)_S = B_T(1 + \gamma_{\rm th}\alpha T). \tag{26}$$

We mention two technical issues regarding the use of the above formulas. First, the calculation of thermodynamic properties at $V(p,T)$ requires $g(\omega; V(p,T))$ or $\omega_j(V(p,T))$, that must be interpolated from the $g(\omega;V)$ or $\omega_j(V)$, known only on the volume grid. GIBBS2 implements two strategies for the interpolation: linear and cubic splines. For the cases we explored, the results are not significantly affected by this choice.

Second, the calculation of $\gamma_{\rm th}$ at very low temperatures is tricky. If equation 23 is used, $\gamma_{\rm th}$ is calculated using a fit to entropy values that approach zero when $T \to 0$, for any volume. If equation 21 is used instead, the quotient is dominated by the lowest frequency modes, i.e. the acoustic branch at gamma that, again, can not be calculated by fitting. The practical solution implemented in GIBBS2 involves extrapolating the results at a very low but not zero temperatures.

3.3 The Debye-Slater model

Even with its intrinsic limitations, the QHA has recently achieved a great deal of success in the prediction of equations of state and thermodynamic properties. However, in spite of the mentioned advances, computing the full vibrational spectra of a crystal on a grid of volumes is still a complex and computationally expensive task. For this reason, simplified models for $g(\omega;V)$ are useful, as they can serve as tools for rapid exploration of the thermal properties of a solid.

A simple and popular[22–24] model of the crystal vibrations dates back to the original work by P. Debye in 1912[25]. The model correctly describes the low and high temperature limits of the constant volume heat capacity. The basis for the model is the observation that, at low temperatures, only low frequency (long wavelength) modes contribute to the heat capacity. These wavelengths are large compared to interatomic spacings, so they see the solid as a continuum, with two transversal and one longitudinal direction-dependent sound velocities. The phonon density of states approximated by the Debye

model is built by treating all phonons as stationary waves in a unstructured solid, and reads:

$$g_{\text{Debye}}(\omega) = \begin{cases} \dfrac{9n\omega^2}{\omega_D^3} & \text{if } \omega < \omega_D \\ 0 & \text{if } \omega \geq \omega_D \end{cases}, \tag{27}$$

where ω_D is the Debye frequency, directly related to the Debye temperature:

$$\Theta_D = \frac{\omega_D}{k_B} = \frac{1}{k_B}\left(\frac{6\pi^2 n}{V}\right)^{1/3} v_0 \tag{28}$$

In the quasiharmonic Debye model, Θ_D is a function of volume, and the Grüneisen ratio is:

$$\gamma_D = -\frac{\partial \ln \Theta_D}{\partial \ln V}. \tag{29}$$

Inserting g_{Debye} into the quasiharmonic formulas yields:

$$F = E_{\text{sta}} + \frac{9}{8}nk_B\Theta_D + 3nk_BT\ln\left(1 - e^{-\Theta_D/T}\right) - nk_BTD(\Theta_D/T) \tag{30}$$

$$S = -3nk_B\ln\left(1 - e^{-\Theta_D/T}\right) + 4nk_BD(\Theta_D/T) \tag{31}$$

$$U = E_{\text{sta}} + \frac{9}{8}nk_B\Theta_D + 3nk_BTD(\Theta_D/T) \tag{32}$$

$$C_v = 12nkD(\Theta_D/T) - \frac{9nk_B\Theta_D/T}{e^{\Theta_D/T} - 1} \tag{33}$$

$$p_{\text{th}} = \frac{\gamma_D}{V}\left[\frac{9}{8}nk_B\Theta_D + 3nk_BTD\left(\frac{\Theta_D}{T}\right)\right] = \frac{\gamma_D U_{\text{vib}}}{V}, \tag{34}$$

where D is the Debye integral:

$$D(x) = \frac{3}{x^3}\int_0^x \frac{y^3 e^{-y}}{1 - e^{-y}}dy. \tag{35}$$

and $U_{\text{vib}} = U - E_{\text{sta}}$ is the vibrational free energy. Incidentally, equation 34 is known as the Mie-Grüneisen equation of state, valid for models where all mode gammas are assigned the same value. In the case of the Debye model, $\gamma_j = \gamma_D$ for all j.

There are a number of ways of calculating the $\Theta_D(V)$ function. Ideally, one would obtain it from the average velocities $v_0(V)$, which in turn can be computed from the transversal and longitudinal velocities using:

$$\frac{3}{v_0^3} = \frac{1}{4\pi}\int d\Omega\left(\frac{2}{v_t^3(\Omega)} + \frac{1}{v_l^3(\Omega)}\right). \tag{36}$$

However, obtaining the sound velocities requires the calculation of the elastic

constants at every volume of the grid, defeating the simplicity purpose of the approximate model.

A reasonable approximation to $\Theta_D(V)$ was originally proposed by Slater[26], implemented in the original GIBBS program[11], and explored in M. A. Blanco's PhD thesis[12]. The Debye temperature is calculated assuming an isotropic solid and $B_S \approx B_{\rm sta}$:

$$\Theta_D = \frac{1}{k_B}\left(6\pi^2 V^{1/2} n\right)^{1/3} f(\sigma)\sqrt{\frac{B_{\rm sta}}{M}}, \tag{37}$$

where M is the molecular mass per primitive cell, and $B_{\rm sta}$ and σ are the static bulk modulus and Poisson ratio at the equilibrium geometry. The $f(\sigma)$ function is:

$$f(\sigma) = \left\{3\left[2\left(\frac{2}{3}\frac{(1+\sigma)}{(1-2\sigma)}\right)^{3/2} + \left(\frac{1}{3}\frac{(1+\sigma)}{(1-\sigma)}\right)^{3/2}\right]^{-1}\right\}^{1/3}. \tag{38}$$

In figure 1, the approximated $g(\omega)$ of the Debye-Slater model are represented along with the calculated phDOS at the experimental volume. For the crudeness of the model, the extent and steepness of the parabola being determined solely using the static energy, the match is quite remarkable. Indeed, as we will see below, the leading error in this model is not in the approximated $g(\omega)$ but in the treatment of the quasiharmonicity.

The Poisson ratio can be calculated *ab initio* or taken as experimental input. A reasonable approximation, and the default value in GIBBS2 is $\sigma = 1/4$, corresponding to a Cauchy solid.

Using equation 37 leads to a Grüneisen ratio:

$$\gamma_{\rm th} = \gamma_S = -\frac{1}{6} + \frac{1}{2}\frac{dB_{\rm sta}}{dp}, \tag{39}$$

where $B_{\rm sta}$ is the static bulk modulus. This expression is known in the literature as the Slater gamma[27,28].

3.4 The Debye-Grüneisen model

Figure 2 shows the Grüneisen ratio in the Slater approximation, calculated using the full QHA and the experimental result. Even for a system as simple as MgO, γ_S differs from the experimental or from the reference QHA result by a non-negligible factor. The cause of this discrepancy was pointed out by

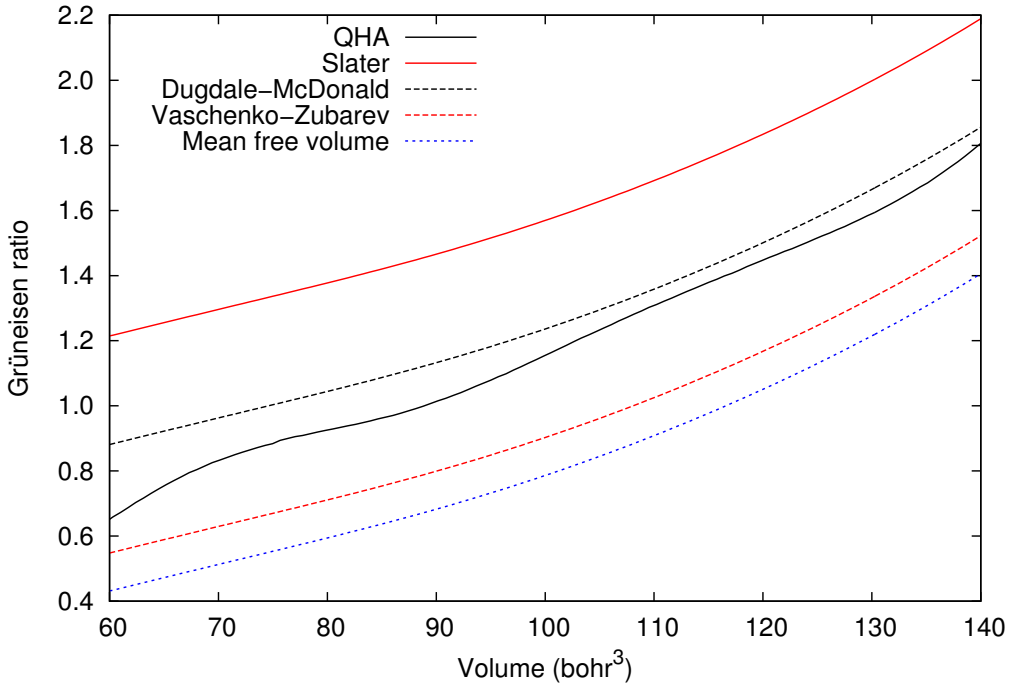

Fig. 2. Different approximations to the Grüneisen ratio are represented against cell volume for magnesium oxide. The curve labeled QHA corresponds to a full quasiharmonic calculation.

Slater[26]: in equation 29, the Poisson ratio is assumed to be invariant with volume. Therefore, quasiharmonicity is not properly introduced in the Debye-Slater model.

In the Debye-Grüneisen model[29], $\Theta_D(V)$ is calculated at the static equilibrium volume V_0 using equation 29. Then, an approximate Grüneisen ratio is chosen to be of the form:

$$\gamma = a + b\frac{dB_{\rm sta}}{dp} = a - b\frac{d\ln B_{\rm sta}}{d\ln V}, \tag{40}$$

that is consistent with some approximate $\gamma_{\rm th}$ proposed in the literature[27,28], including the expressions by Dugdale-McDonald ($a = -1/2, b = 1/2$), Vaschenko-Zubarev ($a = -5/6, b = 1/2$), and the mean free volume gamma ($a = -0.95, b = 1/2$). The Slater gamma is also represented by eq. 40 with $a = -1/6$ and $b = 1/2$.

It is easy to prove that, assuming a $\gamma_{\rm th}$ of the form above is equivalent to setting the volume variation of the Debye temperature to:

$$\Theta_D(V) = \Theta_D(V_0)\frac{(B_{\rm sta}/B_0)^b}{(V/V_0)^a}, \tag{41}$$

where V_0 and B_0 are the static equilibrium volume and bulk modulus respectively. Therefore, by using equation 41 to calculate $\Theta_D(V)$ at arbitrary

volumes introduces a new volume dependence of the Poisson ratio, fixing to some extent the problems in the treatment of the quasiharmonicity.

Indeed, figure 2 shows that approximate $\gamma_{\rm th}$ improve the agreement with the QHA result with respect to γ_S. It is important to note that the amount of theoretical data required is the same as in the Debye-Slater model: the static $E(V)$ and possibly the Poisson ratio at the equilibrium geometry.

3.5 The Debye-Einstein model

The shortcomings of the Debye model are apparent in molecular and loosely packed systems. In these solids, there is a large number of optic branches, that are incorrectly treated as acoustic in the Debye model. Therefore, it comes as no surprise that mixed acoustic/optic approximations to $g(\omega)$ are very popular within the mineralogist community[30,31]. The simplest approach, implemented in GIBBS2, consists of using single frequencies to represent each of the $3n-3$ optic branches[31], and renormalizing the Debye temperature to the 3 acoustic branches:

$$g_{\rm DE}(\omega) = \begin{cases} \dfrac{9n\omega^2}{\omega_{DE}^3} & \text{if } \omega < \omega_{DE} \\ \sum_{j=1}^{3n-3} \delta(\omega - \omega_j) & \text{if } \omega \geq \omega_{DE} \end{cases}, \tag{42}$$

where the normalization condition (eq. 12) yields a Debye-Einstein characteristic temperature (Θ_{DE}) related to the plain Debye model (Θ_D) by:

$$\Theta_{DE} = \frac{\Theta_D}{n^{1/3}} = \frac{6\pi^2}{V} v_0 \tag{43}$$

In GIBBS2, Θ_D is calculated as in the Debye-Slater model, resulting in a new Debye temperature that is correctly independent of the number of atoms in the cell.

Using equation 42 in the QHA expressions yield thermodynamic properties

that average acoustic and optic terms:

$$\begin{aligned} F &= E_{\mathrm{sta}} \\ &+ \underbrace{\frac{9}{8}k_B\Theta_{DE} + 3nk_BT\ln\left(1-e^{-\Theta_{DE}/T}\right) - nk_BTD(\Theta_{DE}/T)}_{F_{\mathrm{ac}}} \\ &+ \underbrace{\sum_{j=1}^{3n-3}\frac{\omega_j}{2} + k_BT\ln\left(1-e^{-\omega_j/k_BT}\right)}_{F_{\mathrm{op}}} \end{aligned} \tag{44}$$

$$\begin{aligned} S &= \underbrace{-3nk_B\ln\left(1-e^{-\Theta_{DE}/T}\right) + 4nk_BD(\Theta_{DE}/T)}_{S_{\mathrm{ac}}} \\ &+ \underbrace{\sum_{j=1}^{3n-3} -k_B\ln\left(1-e^{-x_j}\right) - \frac{\omega_j}{T}\frac{1}{e^{x_j}-1}}_{S_{\mathrm{op}}} \end{aligned} \tag{45}$$

$$U = E_{\mathrm{sta}} + \underbrace{k_BT\left[\frac{9}{8}x_{DE} + D(x_{DE})\right]}_{U_{\mathrm{ac}}} + \underbrace{k_BT\sum_{j=1}^{3n-3}\left[\frac{x_j}{2} + \frac{x_j}{1-e^{-x_j}}\right]}_{U_{\mathrm{op}}} \tag{46}$$

$$C_v = \underbrace{12nk_BD(\Theta_{DE}/T) - \frac{9nk_B\Theta_{DE}/T}{e^{\Theta_{DE}/T}-1}}_{C_{v,\mathrm{ac}}} + \underbrace{nk_B\sum_{j=1}^{3n-3}\frac{(\omega_j/T)^2e^{\omega_j/T}}{(e^{\omega_j/T}-1)^2}}_{C_{v,\mathrm{op}}}. \tag{47}$$

The Grüneisen ratio is calculated as:

$$\gamma_{\mathrm{th}} = \frac{\gamma_S C_{v,\mathrm{ac}} + \gamma_{\mathrm{op}} C_{v,\mathrm{op}}}{C_v} \tag{48}$$

$$\gamma_{\mathrm{op}} = \frac{9B_{\mathrm{sta}}(dB_{\mathrm{sta}}/dp - 1) + 2p_{\mathrm{sta}}}{6(3B_{\mathrm{sta}} - 2p_{\mathrm{sta}})}, \tag{49}$$

and the thermal pressure is:

$$\begin{aligned} p_{\mathrm{th}} &= \underbrace{\frac{\gamma_S}{V}\left[\frac{9}{8}nk_B\Theta_{DE} + 3nk_BTD(\Theta_D/T)\right]}_{p_{\mathrm{ac}}} + \underbrace{\frac{\gamma_{\mathrm{op}}}{V}\sum_{j=1}^{3n-3}\left(\frac{\omega_j}{2} + \frac{\omega_j}{e^{\omega_j/k_BT}-1}\right)}_{p_{\mathrm{op}}} \\ &= \frac{U_{\mathrm{ac}}\gamma_S}{V} + \frac{U_{\mathrm{op}}\gamma_{\mathrm{op}}}{V} \end{aligned} \tag{50}$$

The implementation in GIBBS2 follows that of Fleche[31], where the frequencies at the Γ point calculated, $\omega_i(\Gamma)$ are used as representatives of the whole branch. The input required is further reduced by using only the $\omega_i(\Gamma)$ calculated at the static equilibrium structure and setting the volume evolution of

these frequencies to:

$$\omega_i(\Gamma) = \omega_i^0(\Gamma) \left(\frac{V}{V_0}\right)^{1/6} \left(\frac{B_{\rm sta}}{B_0}\right)^{1/2} \left(1 - \frac{2}{3}\frac{p_{\rm sta}}{B_{\rm sta}}\right)^{1/2}, \tag{51}$$

where $\omega_i^0(\Gamma)$ are the frequencies at Γ corresponding to the equilibrium, $p_{\rm sta}$ and $B_{\rm sta}$ are the static pressure and bulk modulus and V_0 and B_0 are the static equilibrium volume and bulk modulus.

To summarize this section, we have added to the GIBBS2 code the possibility of using four models. In increasing order of complexity and accuracy: Debye-Slater, Debye-Grüneisen, Debye-Einstein and the full QHA.

4 Energy fitting

In the previous article[13], we exhaustively explored how different equations of state yield diverging properties when fitted to the same static $E(V)$ dataset. We discussed how an average of strain polynomials can not only render more accurate equilibrium volume, bulk modulus,... but also offer an insight into the quality of the fit. As an additional benefit, the process of polynomial averaging allows the calculation of error bars for the properties, that are sensitive to the quality of the input data.

The same fitting techniques and EOS expressions as in the ASTURFIT package[13] have been implemented in GIBBS2, including a number of traditional EOS as well as strain polynomials and their averages. The former are fitted using a non-linear minimization algorithm, while for the latter we use the robust linear polynomial fitting methods. Namely, the common EOS subject to non-linear fit in GIBBS2 are:

(1) Birch-Murnaghan (BM) family: non-linear fits up to 4^{th} order.
(2) Poirier-Tarantola (PT) family: non-linear fits up to 5^{th} order.
(3) Murnaghan EOS.
(4) Anton-Schmidt EOS.
(5) Vinet EOS.
(6) Holzapfel's AP2 EOS.

The BM and PT families can be fit as polynomials to arbitrary order using the Eulerian and natural strains respectively. Additional strain choices are: Lagrangian, infinitesimal, V/V_0, $(V/V_0)^{1/3}$ and the simple volume strain (V).

The implementation in GIBBS2 extends the results of ref. [13], to the fitting of $F^*(V;T)$ and $-TS(V;T)$ at any given temperature T. Applying the same

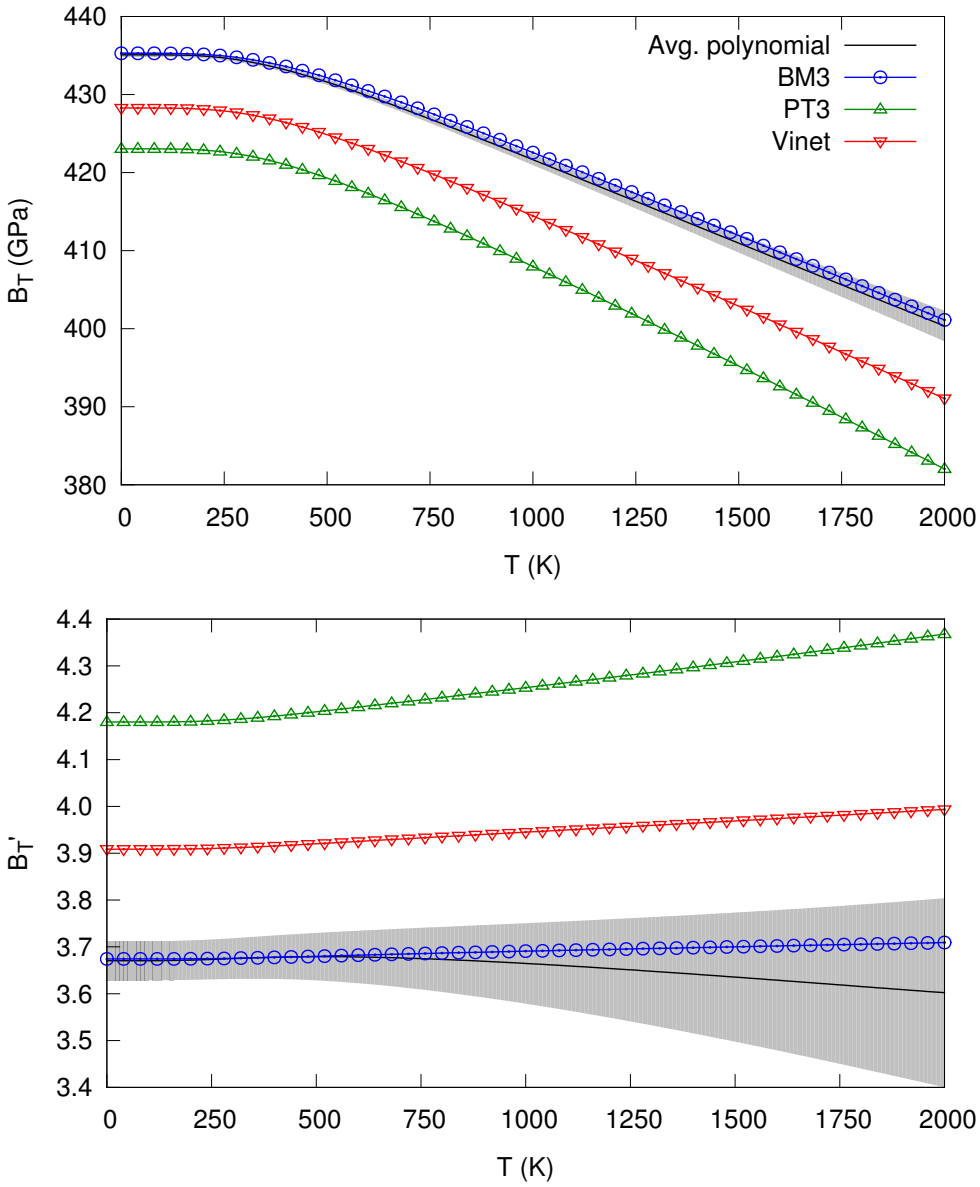

Fig. 3. Isothermal bulk modulus (up) and its pressure derivative (down) for diamond, calculated using different equations of state. The shaded area represents the error bar calculated for the average polynomial.

statistical methods, it is possible to compute error bars to the calculated thermodynamic properties.

A sample of the diverging results obtained by using different equations of state in diamond is shown in figure 3. The third-order Poirier-Tarantola and Vinet EOS, which are routinely used in the literature, diverge from the polynomial average result by several times the calculated error bar. For instance, the isothermal bulk modulus predicted by the popular Vinet EOS is off the average polynomial result by 6.78 GPa, a non-negligible amount. The third-

order Birch-Murnaghan result is within the error bar limits, but experience with other systems suggests that the good behavior of this particular EOS is accidental. It was already discussed in reference [13] that the precision of the calculated properties degrades when these depend on higher order derivatives of the energy. Figure 3 shows a similar trend, even when thermal effects are incorporated. The error bars are comparatively much larger for B'_T than for B_T.

5 Additional capabilities of gibbs2

5.1 Empirical energy corrections

The accuracy of the thermodynamic properties calculated by GIBBS2 is determined by the quality of the underlying energy and vibrational data. In most cases, these data are obtained as a result of a DFT calculation, and the main source of uncertainty is invariably the exchange-correlation functional.

The errors introduced by the functional are systematic, and well studied in the literature. For instance, the accuracy of the calculated thermodynamic properties is greatly improved if a correction is applied to shift the static $E(V)$ curve in a way that the model reproduces the experimental volume and, optionally, the bulk modulus at ambient conditions. We have called empirical energy corrections (EEC) to such energy scalings, and will be explained in detail elsewhere.

Three different corrections to the static energy implemented in GIBBS2:

(1) The PSHIFT EEC:

$$\tilde{E}_{\mathrm{sta}}(V) = E_{\mathrm{sta}}(V) + \Delta p V. \tag{52}$$

(2) The APBAF EEC:

$$\tilde{E}_{\mathrm{sta}}(V) = E_{\mathrm{sta}}(V) + \frac{\alpha}{V}. \tag{53}$$

(3) The BPSCAL EEC:

$$\begin{aligned}\tilde{E}_{\mathrm{sta}}(V) = {} & E_{\mathrm{sta}}(V_0) \\ & + \frac{B_{\mathrm{exp}} V_{\mathrm{exp}}}{B_0 V_0} \left[E_{\mathrm{sta}}\left(V \frac{V_0}{V_{\mathrm{exp}}} \right) - E_{\mathrm{sta}}(V_0) \right].\end{aligned} \tag{54}$$

The value of the free parameters Δp, α, V_{exp} and B_{exp} in the three EECs above are chosen so that the experimental room temperature equilibrium volume is reproduced and, in the case of BPSCAL, also the experimental bulk modulus.

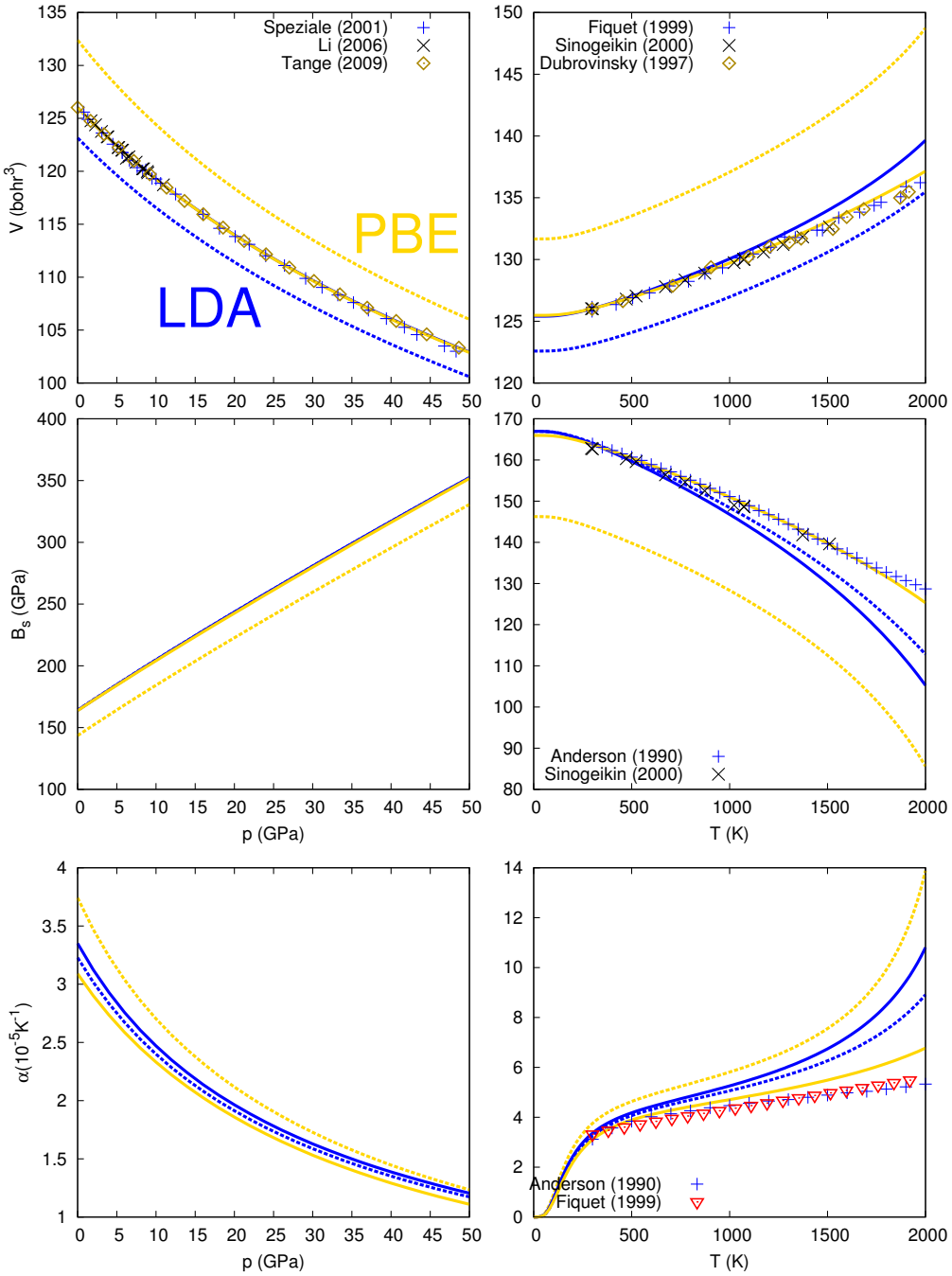

Fig. 4. Calculated pressure and temperature dependence of the volume (up), adiabatic bulk modulus (middle) and thermal expansion coefficient (down) of the B1 phase of MgO, compared to experimental data. Dotted lines represent uncorrected results for the LDA (blue) and PBE (gold) exchange correlation functionals. BP-SCAL-corrected results are shown as full lines. The experimental data correspond to references [32–38] and are labeled using the first author and the year.

Figure 4 illustrates the systematic trends caused by the choice of the exchange-correlation functional. It is well known that solids calculated using LDA tend to be overbound: volumes are too small and bulk moduli too large. Contrarily, PBE tends to underbind. This very effect is displayed in the above figure for magnesium oxide. Using the BPSCAL correction, volumes and bulk moduli are brought to a far better agreement with experimental results than the bare DFT results. In addition, the limit of validity of the harmonic approximation, that breaks down at high temperature, is pushed to higher temperatures, especially for the PBE functional.

5.2 Electronic contributions to the free energy

Apart from the vibrational, some solids possess additional degrees of freedom that contribute to the free energy. For instance, in a metal, electrons are free to traverse the solid because the band structure contains electronic levels at energies arbitrarily close to the Fermi level. There is an electronic contribution $F^*_{\rm el}$ to the F^* that is usually small compared to $F^*_{\rm vib}$, except at very low temperatures.

The electronic contribution has been implemented in GIBBS2 in three ways:

(1) The Sommerfeld model of free and independent electrons.
(2) The Sommerfeld model, but the density of states at the Fermi level is obtained from a first principles calculation.
(3) The user supplies polynomial fits to $F^*_{\rm el}(T)$ and $-TS_{\rm el}(T)$, calculated using the finite-temperature DFT formalism[39].

The expressions for the free energy and entropy for a free electron model are:

$$S_{\rm el} = C_{v,{\rm el}} = \frac{\pi^2}{3} N(\varepsilon_F) k_B^2 T \tag{55}$$

$$F_{\rm el} = -U_{\rm el} = \frac{TS_{\rm el}}{2}, \tag{56}$$

where $N(\varepsilon_F)$ is the density of states at the Fermi level, that in the Sommerfeld model reads:

$$N(\varepsilon_F) = \frac{3}{2}\frac{n_{\rm elec}}{\varepsilon_F}, \tag{57}$$

with $n_{\rm elec}$ the number of valence electrons.

Figure 5 represents the electronic contributions to the entropy and free energy *versus* volume. The results of the first principles calculation agree very well with the free electron model, consistent with the fact that elemental fcc aluminum is a characteristic free-electron-like metal. Also, the free energy and entropy contributions are 3–4 orders of magnitude smaller than the vibrational

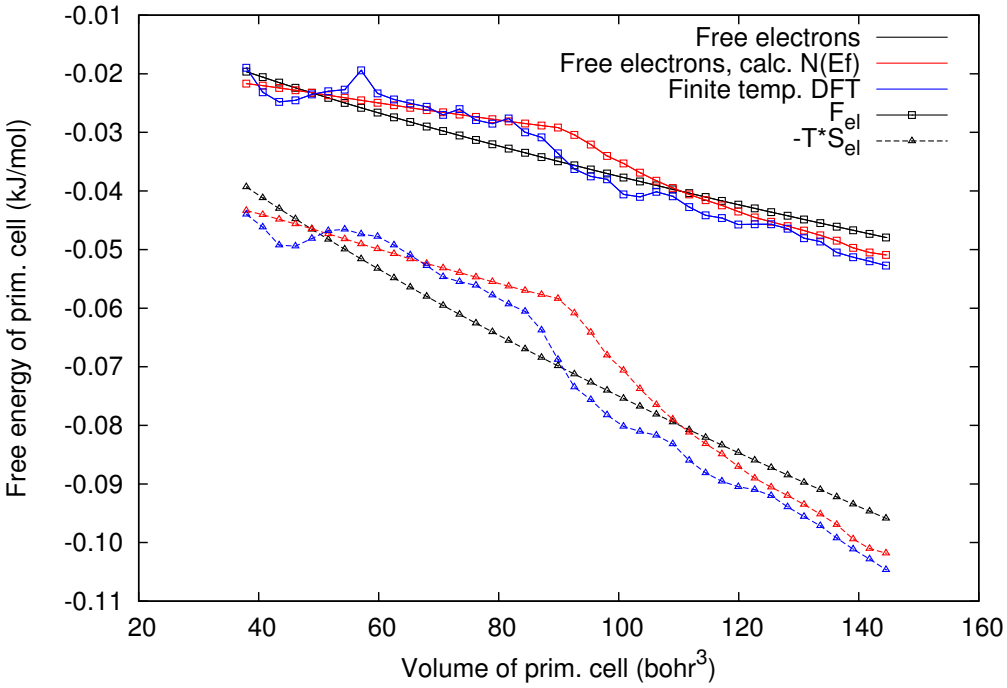

Fig. 5. Electronic Helmholtz free energy and $-TS_{\mathrm{el}}$ is represented against cell volume for fcc Al at room temperature. Note the energy scale is in kJ/mol.

terms, and they do not modify in an appreciable way the calculated thermodynamic properties. Because of the exceedingly small value of the electronic energy compared to the static energy, a certain degree of noise when information from the *ab initio* calculation is obtained, even when a very fine $\boldsymbol{k}$-point mesh is used. In figure 5, for instance, a $52 \times 52 \times 52$ Monkhorst-Pack grid was used.

5.3 Automatic computation of phase diagrams

Different phases of a solid correspond to different local minima and attraction basins of the potential energy surface. A corollary of the principle stated in equation 2 is that, given a pressure and a temperature, the thermodynamically stable phase is that with lowest $G(p, T)$.

In the original GIBBS program, only one $E(V)$ curve and, therefore, only one phase could be treated in a single run. GIBBS2 has been generalized to introduce the possibility of computing the $G(p, T)$ of different phases and detecting the most stable. In addition, transition pressures at any temperature, phase transition volume and G changes and phase diagrams are automatically computed in a simple and straightforward way.

6 The gibbs2 distribution

6.1 Structure of the source code

GIBBS2 is written in Fortran90. The driver routine is the `gibbs2.f90` file, which accesses functions and subroutines contained in ancillary modules (described below). The source code is contained in the `src/` directory of the GIBBS2 distribution. The sequence of tasks in the main routine are:

(1) Read and parse the input file and any auxiliary file. GIBBS2 accepts a single input file, typically with extension `ing`. The input file contains the source $E(V)$ and vibrational data (or a pointer to the files where it can be found), the pressure and temperature list where the properties are calculated and, optionally, keywords controlling the kind of calculation to be run.
(2) Once the reading is finished, the information of each phase is initialized: input units are converted to atomic units, phonon DOS or frequencies are renormalized,...
(3) The empirical energy corrections are applied, if requested.
(4) The static energy is fitted against the volume, and a detailed account of the static equation of state and the static equilibrium properties is reported.
(5) If more than one phase is defined in input, the static transition pressures are calculated.
(6) Once the static computation is finished, the program checks whether any of the phases has an associated thermal model. If they do, then GIBBS2 runs over the temperature-pressure pair list defined by the user, computing the thermodynamic properties at each pair.
(7) Finally, transition pressures at the input temperatures are calculated and reported.

A description of the modules used by `gibbs2.f90` follows. The list is ordered, with the most basic modules first:

param.f90 Contains mathematical and physical constants, enumerates and basic variables and subroutines.
tools.f90 Self-contained subroutines and functions that perform well-defined tasks: input/output, timer, error signalling, string manipulation, memory management, sorting, and mathematical operations.
evfunc.f90 Definitions of the strains and equations of state. The main functions of this module are the `fvn` that, given the information of a fit and a volume calculate the n^{th} derivative of the energy.
fit.f90 Routines for the fitting of energy *versus* volume curves, possibly with

a shifting constant pressure.

varbas.f90 Basic thermodynamic subroutines and variables. The large `phase` user-defined type, containing the description of a phase, is defined here. Provides subroutines for reading and parsing external files and for phase initialization.

gnuplot_templates.f90 A small module defining subroutines for the generation of gnuplot files.

eos.f90 A module containing a single driver routine for static energy fits.

debye.f90 Calculation of thermodynamic properties at a given temperature, for all the defined thermal models.

topcalc.f90 Highest level routines, called directly by the main program.

setvariables.f90 A single subroutine that manipulates GIBBS2 SET options according to the user's input.

In addition, parts of external libraries (obtained from `www.netlib.org`) have been included, namely:

- The routine dgam.f for the computation of the incomplete Gamma function (used in the AP2 equation of state)
- The spline library `pppack`.
- Part of the `minpack` library for the non-linear minimization of functions using a Levenberg-Marquardt algorithm.
- The `slatec` library for the polynomial fits.

6.2 Documentation and tests

The GIBBS2 distribution comes with full documentation and tests. The user's guide can be found in the `doc/` subdirectory, either in plain text, or a compiled pdf file. The tests are located in the `tests/` directory. There are 6 tests that try to extensively display the features of `gibbs2`. These tests access first principles data for the same test cases used in this article: magnesium oxide (phases B1 and B2), fcc aluminum and diamond; calculated using LDA and PBE, under the conditions described in section 2.

6.3 Installation

To compile GIBBS2, simply enter the `src/` directory and modify the `Makefile.inc` file to point to a Fortran90 compiler (the default compiler is `gfortran`). Then, a `make` command builds the program, that can be linked to the user's `bin/`.

7 Test case

7.1 Sample input

A simple input that compares the results of several thermal models in MgO follows. Each thermal model corresponds to one phase, so transition pressures between phases are not computed (`set notrans` option). The number of atoms per primitive cell (2) and the mass of the cell in atomic mass units (40.3044) are needed for the Debye-like models. The pressure/temperature list contains pressures from 0 up to 250 GPa, in steps of 1 GPa, at room temperature (-1). Each thermal model uses the same static $E(V)$ data source, in the file `mgo.res`. The calculated 3 non-zero equilibrium geometry frequencies at Γ are indicated for the Debye-Einstein model.

```
# MgO
set notrans
mm 40.3044
vfree 2
pressure 0 1 250
temperature -1

phase debye file ../dat/mgo_pbe/mgo.res tmodel debye \
                units energy ry freq cm-1 \
                prefix ../dat/mgo_pbe/
phase debgrun file ../dat/mgo_pbe/mgo.res tmodel debye_gruneisen dm \
                units energy ry freq cm-1 \
                prefix ../dat/mgo_pbe/
phase debeins file ../dat/mgo_pbe/mgo.res tmodel debye_einstein \
                units energy ry freq cm-1 \
                prefix ../dat/mgo_pbe/
freqg0 debeins
  402.9580 402.9580 701.1656
endfreqg0
phase qha file ../dat/mgo_pbe/mgo.res tmodel qha \
                units energy ry freq cm-1 \
                prefix ../dat/mgo_pbe/
end
```

The input is saved to `test.ing` and run using:

```
gibbs2 test.ing test.out
```

The execution time is less than 6 seconds.

The file `test.out` is the main output of GIBBS2. A summarized version follows. Ellipsis are denoted by `[...]` symbols.

```
GIBBS2: (p,t) thermodynamics of solids.

  A. Otero-de-la-Roza, V. Lua~na and D. Abbasi.
  See doc/gibbs2.txt for details on the proper citation of \
  this software.
* Input
  Title:
  Output file (lu= 2): stdout
  Units: output is in atomic units, except where noted.
  Number of atoms per primitive cell:   2
  Molecular mass (amu):       40.30440000
  Infinite V energy (hy):   0.000000000000E+00
  Number of phases:   4
  Phase   1: debye
  Phase   2: debgrun
  Phase   3: debeins
  Phase   4: qha
  Polynomial fit mode: slatec
  Polynomial weight mode: gibbs2
  Max. polynomial degree: 12

COMMENT(phase_checkconvex): Found   4 inflection points in (E,V) \
 of phase debye
  Near (E,V) point number ** :     153.0874653
  Near (E,V) point number ** :     153.7787188
  Near (E,V) point number ** :     154.4699723
  Near (E,V) point number ** :     155.1612257
[...]
* Pressure range examined
  Min_phases{p_max} (GPa):     1801.897
  Pressure range (GPa):        0.000 ->      250.000
  Number of p points:    251

* Phase information after initial setup
+ Phase  1 (debye)
  Number of volume points:  174
  Number of vfree units (Z):        1.000
  p(V) input data? F
```

```
  Pressure range (GPa):      -20.406 ->     1801.897
  Number of interpolated fields :    0
  Input units:
    Volume : bohr^3
    Energy : Ry
    Pressure : GPa
    Frequency : cm^(-1)
    DOS energy : Hartree
  Output units are atomic units (Hy), except where noted.
  First/last volume (bohr^3):   \
    4.000000000000E+01    1.600000000000E+02
  First/last energy (Hy):  \
    -7.256282263500E+01   -7.362748155500E+01
  Poisson ratio (sigma):       0.250000
  Poisson function, f(sigma):       0.859949
  Correction of static energy: no correction
  Energy fit mode:   130100
  S(V) fit mode:   130100
  ThetaD(V) fit mode:   130100
  omega(V) fit mode:   130506
  Number of fixed fit parameters:   0
  Static equilibrium volume (bohr^3):       130.0791903025
  Static equilibrium energy (Hy):       -73.6398334037
  Static equilibrium energy (kJ/mol):   -193341.3531454799
  Static bulk modulus (GPa):      150.495329
  Static EOS fit, error RMS (Hy):   4.9714060E-06
  Static EOS fit, max|error| (Hy):   1.2153275E-05
  r2 of the fit:   9.999999306879E-01
  Akaike information criterion:  -3.324033510862E+03
  Bayesian information (Schwarz) criterion:  -3.279806736673E+03
  Temperature model: Debye, Td from static B(V).
  All data points are ACTIVE for dynamic calculations
WARNING(phase_popinfo): Max. pressure (    1801.897) exceeds      500.000

  Fit to static E(V) data:
# Copy in file : test.eos_static
# Lines beginning with 'e' contain fit error estimation.
#    p(GPa)          E (Hy)     V(bohr^3)      V/V0  \
           p_fit(GPa)   B(GPa)         Bp      Bpp(GPa-1)
      0.0000  -7.363983340E+01   130.0792  1.0000000 \
            0.0000   150.4953    4.1284098  -2.6643E-02
e     0.0000   6.942853822E-06     0.0050  0.0000383 \
            0.0000     0.2632    0.0091035   2.2082E-03
[...]
    249.0000  -7.285510749E+01    75.5707  0.5809595 \
```

```
          249.0000   962.7513    2.9588830  -1.2099E-03
e   249.0000   1.907348633E-06     0.0017  0.0000129 \
            0.0000     0.1030    0.0027031   2.0426E-05
    250.0000  -7.285254022E+01    75.4924  0.5803573 \
          250.0000   965.7095    2.9576756  -1.2049E-03
e   250.0000   1.907348633E-06     0.0017  0.0000129 \
            0.0000     0.1037    0.0026941   2.0693E-05
# Polynomial fit to strain:
# Degree : 12
#      p(x) = a_0 + a_1 * f(V) + ... + a_n * f(V)^n
# a_00 =  -7.363982856743E+01
# a_01 =   7.631351488211E-03
# a_02 =   3.010947421871E+00
# a_03 =   3.875836351843E-01
# a_04 =   6.716613773129E-03
# a_05 =  -7.466501037307E+00
# a_06 =   3.413490981977E+01
# a_07 =  -6.053735322551E+01
# a_08 =  -6.024159002718E+01
# a_09 =   4.906434420653E+02
# a_10 =  -9.524557855687E+02
# a_11 =   8.498976616667E+02
# a_12 =  -2.994128654586E+02
# V_scal (bohr^3) =   1.295848475056E+02
# p_scal (GPa) =       0.000000000000

# Composition of the average polynomial and equilibrium static properties:
# n      weight   V(bohr^3)        E(Hy)      B(GPa)   \
                                  Bp      Bpp(GPa-1)
  2    0.0000000   130.7640  -7.363998E+01   149.6773  \
                              4.0000000   -2.5982E-02
[...]
 12    0.1192278   130.0865  -7.363983E+01   150.1951  \
                              4.1237206  -2.3010E-02
 -average pol.--   130.0792  -7.363983E+01   150.4953  \
                              4.1284098  -2.6643E-02
 --dir. average-   130.0792  -7.363983E+01   150.4953  \
                              4.1284076  -2.6636E-02
 ---std. dev.---     0.0050   6.942854E-06     0.2632  \
                              0.0091035   2.2082E-03

+ Phase  2 (debgrun)
[...]
+ Phase  3 (debeins)
[...]
```

```
+ Phase  4 (qha)
[...]

* Input and fitted static energy
  Writing file: test.efit

  Writing file : test_efit.aux

  Writing file : test_efit.gnu

* Plotting static DeltaH

  Writing file : test_dH.aux

  Writing file : test_dH.gnu

* Computed Debye temperatures from static data
+ Phase debye
# ThetaD at static eq. volume:     792.05
# V(bohr^3)  Tdebye(K)   Tdebye_slater(K)
    40.0000    3810.55    3810.55
[...]
   159.3087     512.28     512.28
   160.0000     506.81     506.81
[...]

* Temperature range examined
  Min_{DebyeT} (K):      198.767
  Temperature range (K):      298.150 ->      298.150
  Number of T points:      1

* Calculated temperature effects
  Writing file : test.eos

+ Phase debye
+ Phase debgrun
+ Phase debeins
+ Phase qha

  Writing file: test_all_p.gnu

GIBBS2 ended successfully (  5 WARNINGS,   4 COMMENTS)
```

8 Acknowledgements

The development of this code has been done under financial support from the Spanish Ministerio de Ciencia y Tecnología and the ERDF of the European Union (project no. CTQ2006-02976). AOR is indebted to the Spanish Ministerio de Educación for a FPU grant. DA acknowledges financial support by the Spanish goverment under project no. MAT2006-13548-C02-02. The authors belong to the MALTA group (CSD2007-0045 project, MEC Consolider Ingenio 2010 program).

References

[1] R. M. Wentzcovitch, Y. G. Yu, Z. Wu, Thermodynamic properties and phase relations in mantle minerals investigated by first principles quasiharmonic theory, in: Theoretical and Computational Methods in Mineral Physics: Geophysical Applications, Vol. 71 of Reviews in Mineralogy & Geochemistry, Mineralogical Soc. Amer., Chantilly, VA, USA, 2010, pp. 59–98.

[2] D. Errandonea, C. Ferrer-Roca, D. Martínez-García, A. Segura, O. Gomis, A. Muñoz, P. Rodríguez-Hernández, J. López-Solano, S. Alconchel, F. Sapina, High-pressure x-ray diffraction and ab initio study of Ni2Mo3N, Pd2Mo3N, Pt2Mo3N, Co3Mo3N, and Fe3Mo3N: Two families of ultra-incompressible bimetallic interstitial nitrides, Phys. Rev. B 82 (2010) 174105.

[3] B. Alling, E. I. Isaev, A. Flink, L. Hultman, I. A. Abrikosov, Metastability of fcc-related Si-N phases, Phys. Rev. B 78 (2008) 132103.

[4] D. Porezag, M. R. Pederson, A. Y. Liu, Importance of nonlinear core corrections for density-functional based pseudopotential calculations, Phys. Rev. B 60 (1999) 14132–14139.

[5] D. Marx, J. Hutter, Ab initio molecular dynamics: basic theory and advanced methods, Cambridge University Press, 2009.

[6] M. Allen, D. Tildesley, Computer simulation of liquids, Clarendon Press, 1989.

[7] M. Born, K. Huang, Dynamical theory of crystal lattices, Oxford University Press, USA, 1988.

[8] S. Baroni, S. de Gironcoli, A. Dal Corso, P. Giannozzi, Phonons and related crystal properties from density-functional perturbation theory, Rev. Mod. Phys. 73 (2001) 515–562.

[9] B. B. Karki, R. M. Wentzcovitch, S. De Gironcoli, S. Baroni, First-principles determination of elastic anisotropy and wave velocities of MgO at lower mantle conditions, Science 286 (1999) 1705.

[10] Z. Q. Wu, R. M. Wentzcovitch, K. Umemoto, B. S. Li, K. Hirose, J. C. Zheng, Pressure-volume-temperature relations in mgo: An ultrahigh pressure-temperature scale for planetary sciences applications, J. Geophys. Res. 113 (2008) B06204.

[11] M. A. Blanco, E. Francisco, V. Luaña, GIBBS: isothermal-isobaric thermodynamics of solids from energy curves using a quasi-harmonic Debye model, Comput. Phys. Commun. 158 (2004) 57–72, source code distributed by the CPC program library: `http://cpc.cs.qub.ac.uk/summaries/ADSY`.

[12] M. Álvarez Blanco, Métodos cuánticos locales para la simulación de materiales iónicos. Fundamentos, algoritmos y aplicaciones, Tesis doctoral, Universidad de Oviedo (Julio 1997).

[13] A. Otero-de-la Roza, V. Luaña, Gibbs2: A new version of the quasi-harmonic model code. I. Robust treatment of the static data., Comput. Phys. Commun.(submitted).

[14] P. Giannozzi, S. Baroni, N. Bonini, M. Calandra, R. Car, C. Cavazzoni, D. Ceresoli, G. L. Chiarotti, M. Cococcioni, I. Dabo, A. Dal Corso, S. de Gironcoli, S. Fabris, G. Fratesi, R. Gebauer, U. Gerstmann, C. Gougoussis, A. Kokalj, M. Lazzeri, L. Martin-Samos, N. Marzari, F. Mauri, R. Mazzarello, S. Paolini, A. Pasquarello, L. Paulatto, C. Sbraccia, S. Scandolo, G. Sclauzero, A. P. Seitsonen, A. Smogunov, P. Umari, R. M. Wentzcovitch, QUANTUM ESPRESSO: a modular and open-source software project for quantum simulations of materials, J. Phys.-Condens. Matter 21 (2009) 395502, `http://www.quantum-espresso.org`.

[15] D. Vanderbilt, Soft self-consistent pseudopotentials in a generalized eigenvalue formalism, Physical Review B 41 (1990) 7892–7895.

[16] P. Carrier, R. Wentzcovitch, J. Tsuchiya, First-principles prediction of crystal structures at high temperatures using the quasiharmonic approximation, Phys. Rev. B 76 (2007) 64116.

[17] N. W. Ashcroft, N. D. Mermin, Solid state physics, Thomson Learning Inc., 1976.

[18] X.-J. Chen, C. Zhang, Y. Meng, R.-Q. Zhang, H.-Q. Lin, V. V. Struzhkin, H.-K. Mao, beta-tin – Imma – sh phase transitions of germanium, Phys. Rev. Lett. 106 (2011) 135502.

[19] K. Umemoto, R. M. Wentzcovitch, S. Saito, T. Miyake, Body-centered tetragonal C-4: a viable sp(3) carbon allotrope, Phys. Rev. Lett. 104 (2010) 125504.

[20] B. C. Wood, N. Marzari, Dynamics and thermodynamics of a novel phase of NaAlH4, Phys. Rev. Lett. 103 (2009) 185901.

[21] A. R. Oganov, J. Chen, C. Gatti, Y. Ma, Y. Ma, C. W. Glass, Z. Liu, T. Yu, O. O. Kurakevych, V. L. Solozhenko, Ionic high-pressure form of elemental boron, Nature 457 (2009) 863–867.

[22] X.-R. Chen, Z.-Y. Zeng, Z.-L. Liu, L.-C. Cai, F.-Q. Jing, Elastic anisotropy of epsilon-Fe under conditions at the Earth's inner core, Phys. Rev. B 83 (2011) 132102.

[23] L. Deng, X. Liu, H. Liu, J. Dong, High-pressure phase relations in the composition of albite naalsi3o8 constrained by an ab initio and quasi-harmonic debye model, and their implications, Earth Planet. Sci. Lett. 298 (2010) 427–433.

[24] D. Errandonea, R. S. Kumar, L. Gracia, A. Beltran, S. N. Achary, A. K. Tyagi, Experimental and theoretical investigation of ThGeO4 at high pressure, Phys. Rev. B 80 (2009) 094101.

[25] P. Debye, Concerning the theory of specific heat, Ann. Physik 39 (1912) 789–839.

[26] J. Slater, Introduction to chemical physics, McGraw-Hill, 1939.

[27] J. Poirier, Introduction to the Physics of the Earth's Interior, Cambridge University Press, 2000.

[28] L. Vocadlo, J. Poirer, G. Price, Gruneisen parameters and isothermal equations of state, Am. Mineralog. 85 (2000) 390.

[29] V. L. Moruzzi, J. F. Janak, K. Schwarz, Calculated thermal properties of metals, Phys. Rev. B 37 (1988) 790–799.

[30] S. W. Kieffer, Thermodynamics and lattice vibrations of minerals: 3. Lattice dynamics and an approximation for minerals with application to simple substances and framework silicates, Rev. Geophys. 17 (1979) 35–59.

[31] J. L. Fleche, Thermodynamical functions for crystals with large unit cells such as zircon, coffinite, fluorapatite, and iodoapatite from ab initio calculations, Phys. Rev. B 65 (2002) 245116.

[32] S. Speziale, C. S. Zha, T. S. Duffy, R. J. Hemley, H. K. Mao, Quasi-hydrostatic compression of magnesium oxide to 52 GPa: Implications for the pressure-volume-temperature equation of state, J. Geophys. Res. 106 (2001) 515–528.

[33] B. Li, K. Woody, J. Kung, Elasticity of MgO to 11 GPa with an independent absolute pressure scale: Implications for pressure calibration, J. Geophys. Res. 111 (2006) B11206.

[34] Y. Tange, Y. Nishihara, T. Tsuchiya, Unified analyses for PVT equation of state of MgO: A solution for pressure-scale problems in high PT experiments, J. Geophys. Res. 114 (2009) B03208.

[35] G. Fiquet, D. Andrault, J. P. Iti, P. Gillet, P. Richet, X-ray diffraction of periclase in a laser-heated diamond-anvil cell, Phys. Earth Planet. Int. 95 (1996) 1–17.

[36] S. V. Sinogeikin, J. M. Jackson, B. O'Neill, J. W. Palko, J. D. Bass, Compact high-temperature cell for brillouin scattering measurements, Rev. Sci. Instrum. 71 (2000) 201–206.

[37] L. S. Dubrovinsky, S. K. Saxena, Thermal Expansion of Periclase (MgO) and Tungsten (W) to Melting Temperatures, Phys. Chem. Minerals 24 (1997) 547–550.

[38] O. Anderson, K. Zou, Thermodynamic functions and properties of MgO at high compression and high temperature, J. Phys. Chem. Ref. Data 19 (1990) 69–83.

[39] N. D. Mermin, Thermal properties of the inhomogeneous electron gas, Phys. Rev. 137 (1965) A1441–A1443.